NSF-DMR-0821224
Development of a full-Muller-matrix spectroscopic ellipsometer for far-IR radiation at the National Synchrotron Light Source

Abstract: A far-IR spectroscopic ellipsometer has been developed and installed at the U4IR beamline of the National Synchrotron Light Source (NSLS) in Brookhaven National Laboratory (BNL). The main application of this ellipsometer system is for thin ferroelectric films, multiferroic materials, anisotropic single crystals, and samples with $\mu \neq 1$. Starting Jan 2011, this instrument is open for general user access. This ellipsometer is capable to measure a full-Mueller matrix $\hat{M}_{ij}$ of the sample by adopting Hauge's method using rotating compensators and rotating wire-grid linear polarizers. An exceptional brightness of synchrotron radiation allows for spectroscopic measurements in a broad spectral range between 10 and 4,000 cm^{-1}. Fourier-transform infrared (FT-IR) spectrometer is used for multi-wavelength data acquisition. LabView software controls the polarizers, sample motors, temperature controllers, and spectrometer. This software allows automated experiments with the pre-programmed measurement schedules.

Introduction

Full-Muller-matrix spectroscopic ellipsometer is designed and developed for applications in the far-infrared (IR) spectral range using synchrotron radiation at the National Synchrotron Light Source (NSLS-BNL). The main goal of our development effort is to create a multiuser facility, which provides experimental support for fundamental questions about the light propagation in materials with $\mu \neq 1$, magneto-electric coupling in novel materials systems, such as multiferroics and meta-materials. This Project is a collaborative effort between NJIT, Rudolph Technologies, Inc., and BNL. PI: A. A. Sirenko, co-PI's: T. Zhou (NJIT), M. Kotelyanskii (Rudolph Technologies), and C. L. Carr (BNL). There are several design features, which make this new facility unique.

1. The main one is an extension of the spectral range to far-IR, between 10 and 700 cm^{-1}. In our Project this extension is facilitated by the properties of the VUV beamlines at NSLS-BNL, which is one of the best synchrotron light sources in the World for the far-IR spectral range. High brightness of the source in the frequency range between 10 and 700 cm^{-1} is crucial for the future applications of the developed instrument. Material studies usually require a broader spectral range with simultaneous capabilities in THz and mid-IR spectral ranges. Correspondingly, our optical design can provide this opportunity for the extended spectral range up to 4,000 cm^{-1} with the use of the interchangeable sets of polarizers, retarders, beamsplitters, and detectors.
2. Another important requirement is to have a small spot size of the focused radiation on the sample. In our design it is facilitated by the use of parabolic mirrors (dispersion-free), which focus synchrotron radiation to a spot-size of a few millimeters. The light source is diffraction-limited in the far-IR spectral range (below 1000 cm^{-1}). For ultra-small sample we developed an option to use 15× focusing objectives, which facilitate transmission polarimetry experiments.
3. As for every ellipsometer, the mechanical stability and reproducibility of the measurements is crucial for data acquisition and analysis. In our design, mechanical stability is provided by the properties of HUBER XYZ+3-circle-goniometer assembly. The whole instrument is controlled by a single Labview program.
4. An important feature of our Project is development of Theory of Operations, Data Analysis, and Data Simulation/Fitting for full-Muller-matrix measurements of dielectric and magnetic properties of various materials.

In the following we will describe details for the Project components and will present our recent accomplishments. The main results are summarized in the invited talk at the 5th International Conference on Spectroscopic Ellipsometry [1]. The theory of the data analysis and simulations in materials with $\mu \neq 1$ is published in Ref.[2]. The principles of the rotatable broad-band optical retarders are published in [3]. The theory of the optical spectra analysis for samples with $\mu \neq 1$ is submitted for publications [4].

1. General design and setup description

The general design of the ellipsometer has been presented in the original Proposal. There was no major change in the design concept. **Figure 1.1** shows our ellipsometer at U4IR beamline, which consists of three major sections:

1. Polarization State Generation (PSG) section.
2. Sample Stage with a cryostat, Theta-Chi rotation, and X-Y-Z translation capability.
3. Polarization State Analyzer (PSA) section.

General Configuration and incorporation to U4IR beamline at NSLS-BNL.

Ellipsometer is installed at the U4IR beamline with parameters listed in **Table I**. This beamline is specialized in development of new instrumentation and beamline systems for eventual implementation at operating IR beamlines, microscopy and high-field magnets, beam stabilization, and ellipsometry [5]. The spokesperson for U4-IR beamline is one of the co-PIs of our Project, G. L. Carr. The parameters of U4IR beamline determine the capabilities of the Ellipsometer. Synchrotron radiation is conditioned with 90 mrad by 90 mrad collection and beam transfer optics based on matched ellipsoidal pair to produce 1:1 image of source through 11 mm aperture diamond window. Synchrotron radiation passes through the Bruker 66v FTIR spectrometer with full complement of beamsplitters. Then the radiation enters the PSG chamber of Ellipsometer. The general view of Ellipsometer is shown in **Fig. 1.1**.

Table I. Characteristics of U4IR beamline.

Spectral Range	Instrument	Spectral Resolution	Greater than Globar	Spot Size (mm)	Total Angular Acceptance (mrad)
2 meV to 2.5 eV	Interferometer (temporary)	0.03 meV	Brightness 100X-1000X that of 1200K thermal source	Diffraction limited	90H x 90V

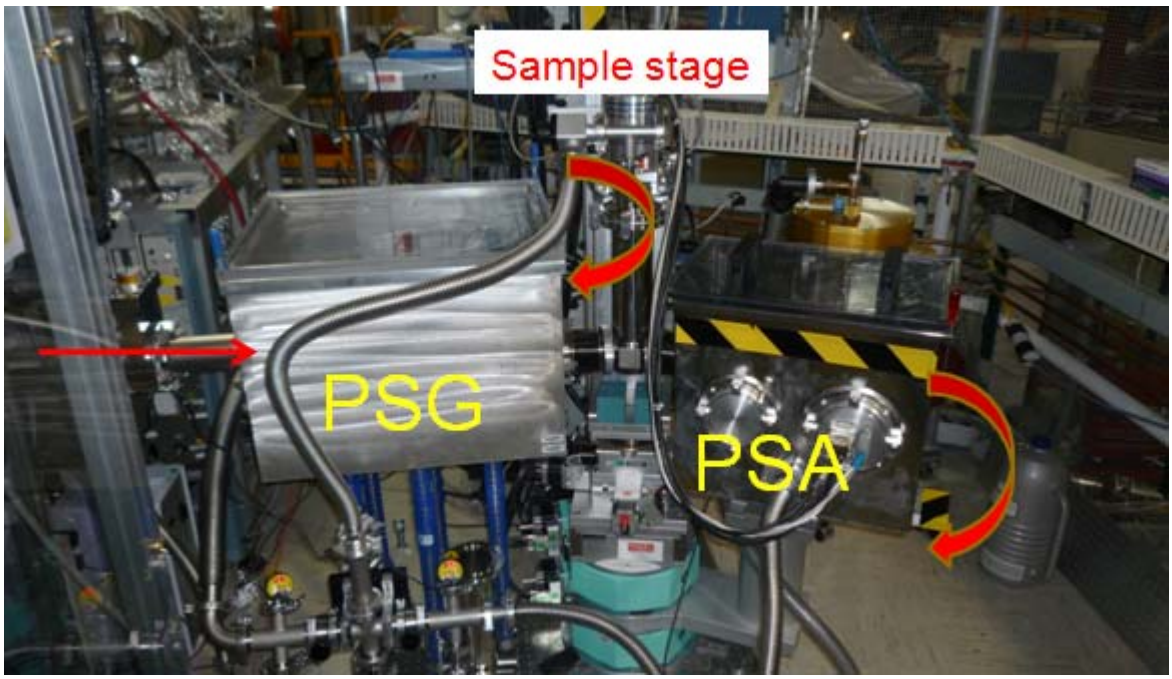

FIG. 1.1 Ellipsometer at U4IR beamline consists of three major components: Polarization State Generation (PSG) section, Sample stage with an optical cryostat, and Polarization State Analyzer (PSA) section. Straight red arrow shows light propagation direction from interferometer towards Ellipsometer. Sample Stage and PSA section can rotate to accommodate the variable AOI measurements.

Vacuum solutions To minimize synchrotron light absorption in the atmosphere, the optical path for the entire system that includes Ellipsometer, interferometer, detector, and the beamline itself is kept under raw vacuum ~ 1 Torr. A gate vacuum valve allows separation between the interferometer and Ellipsometer for independent service, exchange, of the beam splitters and samples. Several vacuum meters are installed for all chambers: PSA, PSG, and Sample Stage. Manifold allows for independent vacuum control of each Ellipsometer component [see **Fig. 1.2(a)**]. Optical cryostat is connected to an Oerlikon turbo-pump station, which provides high vacuum of ~10^{-6} Torr in the sample volume.

Optical windows A pair of optical windows separate three sections of Ellipsometer: PSG, Sample Stage, and PSA. The stationary cryostat windows, which are mounted on the walls of PSG and PSA sections, have a constant orientation with respect to the direction of the synchrotron beam. The window material is 6 micron-thick Mylar. This material is fragile. Its application requires simultaneous vacuum pumping on both sides of the window: ~ 1 Torr at the PAG and PSA sides and 10^{-6} Torr at the Sample side. Flexible bellow connectors, which were customized and ordered from MDC (see **Fig. 1.3**) allow to change the angle of incidence (AOI) for the sample in the range of +/- 7 deg without breaking the sample vacuum.

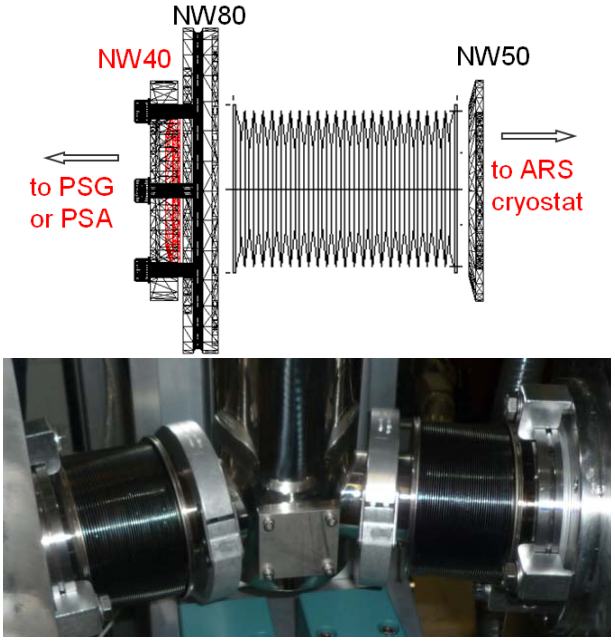

FIG. 1.3 Top panel shows flexible bellow with a window mount on the left-hand side. Bottom panel shows two bellow connections between PSG (left), Sample Stage (center), and PSA (right) sections of Ellipsometer.

FIG. 1.2 (a) Manifold for the vacuum control of the Ellipsometer chambers. (b) Oerlikon turbo-pump station for the Sample Stage and for Bolometer.

Sample Stage

Quality of ellipsometric measurements greatly depends on stability of the sample inside the setup, which is provided by the θ-2θ, χ, and X-Y-Z mechanical controls for the sample position using HUBER components [see **Fig. 1.4(a,b)**]. This system allows for an automatic control for the AOI values during measurements and calibration procedures. The sample motors have a broad range (+/- 20 mm) of the X-Y-Z sample displacements. The stable mechanical design provides reproducibility of the sample motion. The Sample Stage has been designed using standard HUBER components and has a single unit controller for computer communication with the instrument. In **Fig. 1.4(a)** one can see the motorized stages for the sample motion along θ, χ, and X-Y-Z directions and the 2θ arm, which supports the PSA section of the instrument.

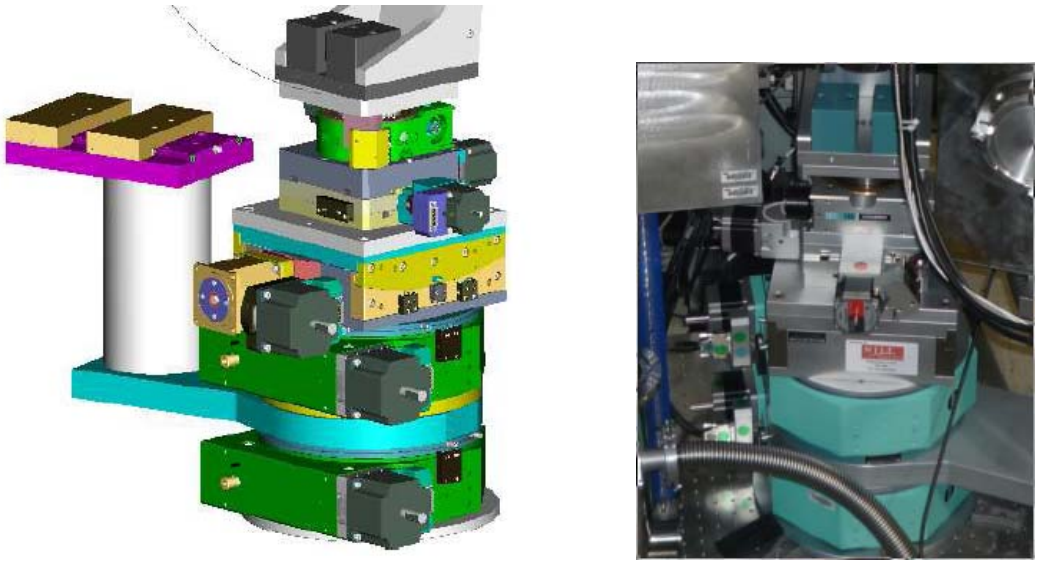

(a) (b)

Fig. 1.4 Schematics of the Sample Stage. (a) CAD drawing for HUBER XYZ+3-circle-goniometer assembly. (b) Photograph of the sample stage assembly.

Low Temperatures / Optical Cryostat

Studies of the phase transitions in strongly correlated materials systems usually require low temperatures for the sample. In our Ellipsometer, two cryostats, OXFORD and ARS, can be used interchangeably for the sample cooling. Both cryostats belong to the "cold-finger" type with the sample positioned on a cupper block in high vacuum. The sample is mounted on a 4 mm-diameter copper holder and is surrounded by two cold shields. Temperature of the sample is measured with a Si diode sensor connected to one of the two Temperature Controllers: Lakeshore or OXFORD. Temperature controllers are integrated into the LabView Program for experiment control. By design, no cold optical windows are used in our cryostats. Note that stationary cold windows mounted on the sample stage would rotate concurrently with the sample and, consequently, they would have a variable AOI on their surface resulting in systematic errors of the ellipsometric measurements.

ARS cryostat This closed-cycle system allows sample temperature variation between 4.2 and 450 K. This system does not require LHe. Cooling is provided with a He compressor [see **Fig. 1.5(a,b)**]. The initial cooling time from 300 K to 5K is about 3 hours. Our decision for the choice of this system *vs*. traditional liquid-helium cryostats is justified by the increasing cost of LHe and related inconveniences at the multiuser facility. Two requirements have been realized in the customized design: (a) quick sample exchange and (b) stationary position of the cryostat windows for a broad range of rotation for the sample. The first solution is illustrated in **Figure 1.5(a)**. The CAD drawing shows the cryostat in the 45-deg position on top of the HUBER XYZ+3-circle-goniometerassembly. This construction allows sample exchange time to be a "one-person procedure" that takes less than 10 min (excluding, of course, the warm-up, pump-down, and cool-down time intervals). One of disadvantages of ARS system is vibration that is transmitted from the compressor to the bolometer trough the metal parts of Ellipsometer. This vibration results in a significant 60 Hz noise on the bolometer that can be detrimental for ellipsometric measurements of weak signals. For example, ellipsometry data for small samples in the far-IR spectral range can be affected by this noise. Possible solutions are related to the use of (i) high scanning speed of Interferometer, (ii) high-pass electronic filter between the bolometer and Interferometer input.

OXFORD cryostat This continuous LHe flow system allows sample temperature variation between 4 K and 300 K (see **Fig. 1.5(c)**]. Cooling is provided with a LHe flow through a transfer line. The initial cooling time from 300 K to 5K is ~0.5 hour. The LHe consumption is between 5 and 10 liters per day. The system is free of vibrations and is preferable for measurements of small samples in the far-IR spectral range.

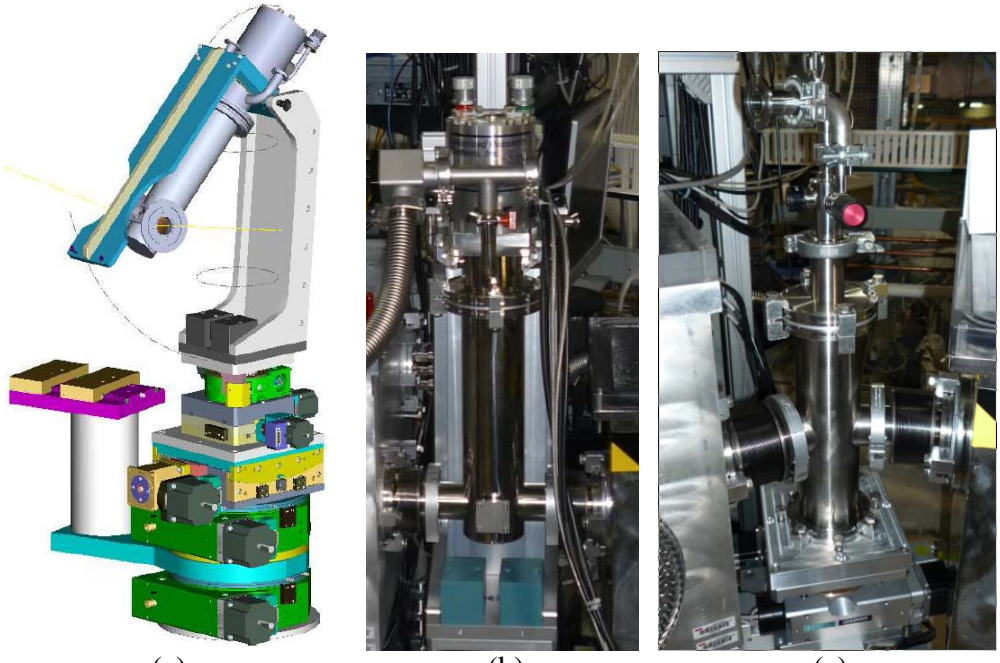

(a) (b) (c)

FIG. 1.5 Schematics of the sample stage and the cryostat assembly .(a) CAD drawing for HUBER XYZ+3-circle-goniometer assembly with the ARS cryostat. The sample exchange position for the cryostat is shown. (b) ARS cryostat . (c) OXFORD cryostat

2. Optical design and optical components

Optical schematic of Ellipsometer is shown in **Fig. 2.1(a)**. To obtain ellipsometric data, synchrotron radiation passes Interferometer, after that is enters PSG section and the desired state of polarization is created with the help of rotating linear polarizers and a retarder. Then, polarized radiation reflects from the sample inside Sample Stage. Later on, the modified light polarization is analyzed inside PSA section with the help of rotating retarder and linear polarizer. Finally, the radiation is focused on the bolometer with the help of a 90 deg parabolic mirror [see **Fig. 2.1(b)**]

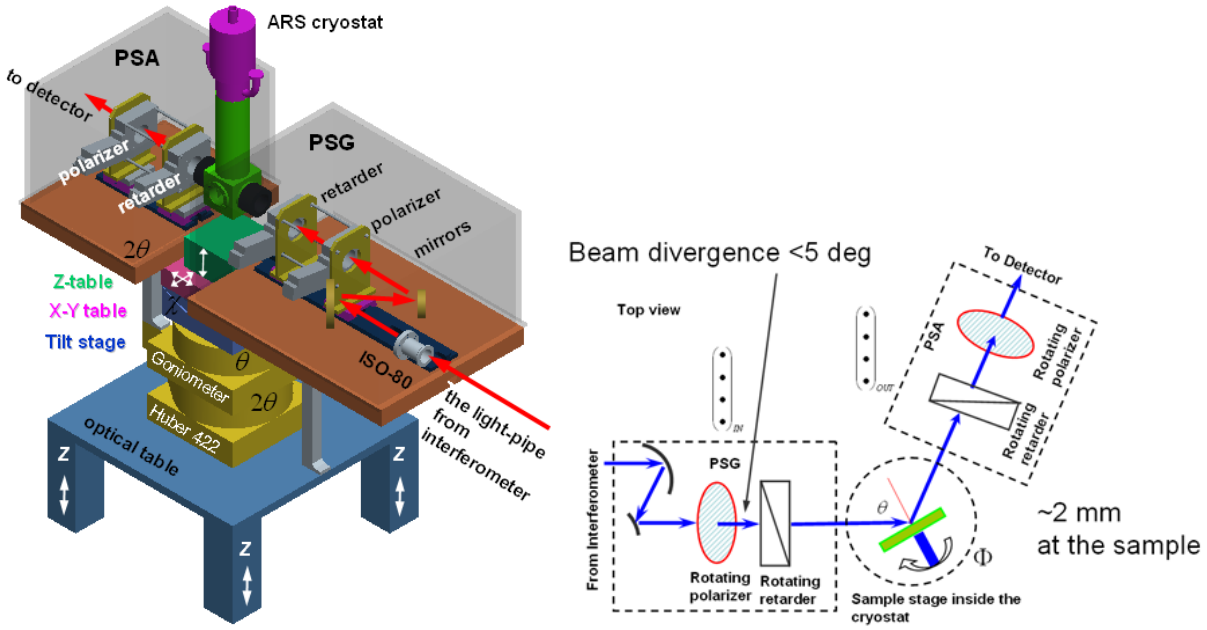

(a) (b)

Fig. 2.1 (a) 3D CAD schematics of the far-IR Ellipsometer in the standard configuration, which consists of PSG and PSA sections, sample stage (ARS or OXFORD optical cryostat and HUBER positioning system) The optical cryostat is mounted on the θ- table of the goniometer. The PSA section and bolometer are mounted on the 2θ-arm of the goniometer. The PSG optical section of the Ellipsometer shares the raw vacuum with the interferometer.
(b) Schematics of a full-Muller matrix ellipsometer with rotating polarizers and retarders in the PSG and PSA sections. Linear polarization of the synchrotron radiation is defined by an additional polarizer (not shown) and a bolometer (detector) is assumed to be polarization insensitive. The sample stage accommodates a variety of incident angles θ along with the angle Φ for sample rotation around the normal-to surface axis The fat dots in the brackets indicate the Stokes parameters that can be generated (S_{IN}) and analyzed (S_{OUT}).

Light focusing

The starting conditions for light focusing are the following: the synchrotron beam has 40 mm in diameter after exiting the BRUKER interferometer. A single off-axis parabolic mirror in a combination with two other flat mirrors is used for the light focusing on the sample [see **Fig. 2.2(a)**]. This beam is "slowly" focused on the sample within the angle of less than 4 deg. The latter requirement is needed to (i) minimize depolarization on the linear polarizer and retarder surfaces and (ii) minimize the uncertainty in the value of the angle of incidence (AOI). The ZEMAX simulation for the light propagation through PSG section is shown in **Figure 2.2(b)**. The long optical path between the entrance and exit of the PSG section provides slow focusing on the sample. Two flat mirrors take care on the small height difference between the beam position and the sample section. All mirrors are supported by the stable gimbal kinematic mounts. The last flat mirror [low left corner in **Fig. 2.2 (b)**] has two motors for automatic alignment in both vertical and horizontal planes. The PSA section is shown in **Figure 2.3(b).**

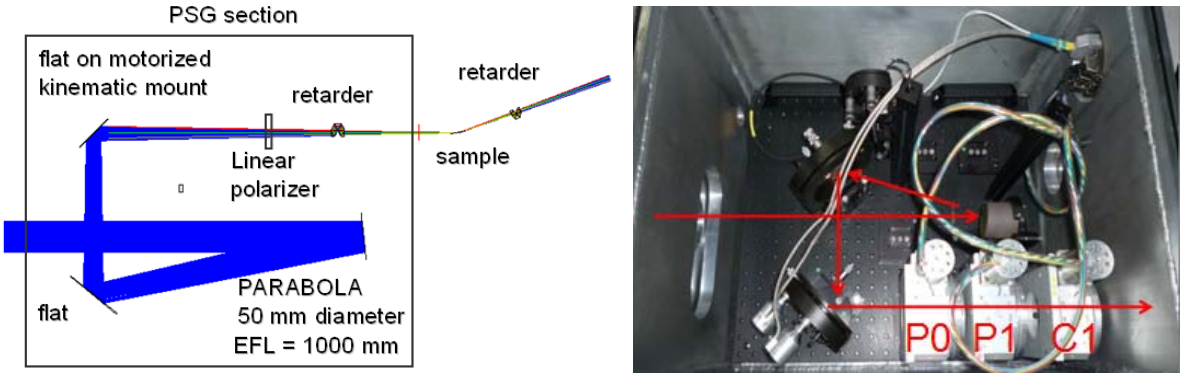

(a) (b)

Fig. 2.2 (a) ZEMAX simulation for the PSG section of Ellipsometer (bottom view). PSG section consists of retarder, linear polarizer, and three mirrors: two flat and one off-axis parabola.
(b) Top view of PSG section. Two polarizers are marked P0 and P1, retarder is marked C1.

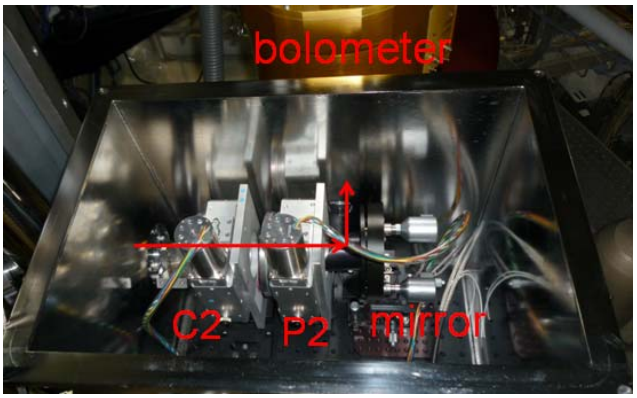

(a) (b)

Fig. 2.3 Top view of PSA section. Polarizer is marked P2 and retarder is marked C2. The light propagation direction is shown with red arrows. Last focusing mirror has two motors for automatic alignment.

Microscope attachment

Measurements of small samples with cross section dimension of ~ 1 mm^2 are very difficult in conventional reflection configuration. However, we develop a microscope attachment for polarimetry measurements in transmission configuration. **Figure 2.4** shows the optical schematics for the microscope attachment. The inset shows focused synchrotron beam at the sample position inside Sample Stage. Two 15× objectives can be placed before and after the sample to bring the size of the focused beam to sub-mm scale. The gold-mirror objectives practically do not affect the light polarization. The attenuation ratio for objectives is fairly high: ~30%, which allows an overall enhancement of the transmitted flux compared to unfocused configuration. Note that without the objectives the beam size at the sample position is about 25 mm^2, which would otherwise result in a 1:25 attenuation for a 1 mm^2 sample.

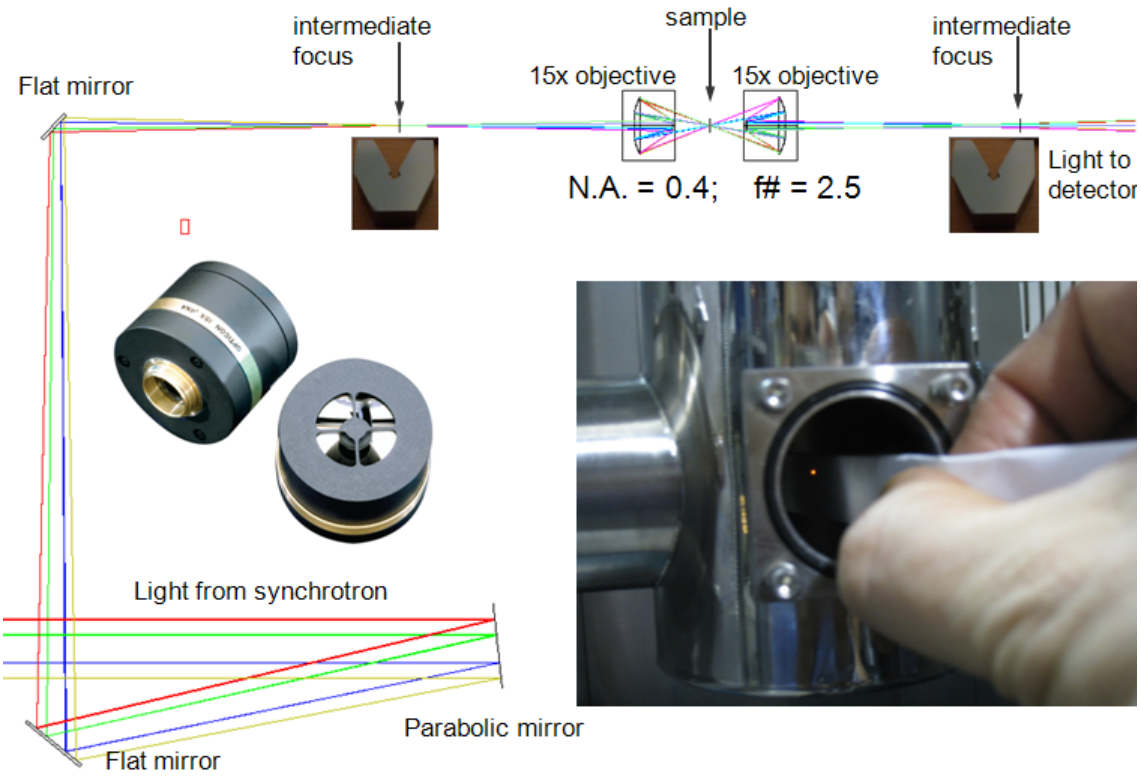

FIG. 2.4 Microscope attachment for transmission polarimetry measurements, which consists of two 15x Schwarzschild objectives. Objectives can be mounted inside the cryostat vacuum shroud. Inset shows light focusing at the sample position.

3. Linear Polarizers and Retarders

To support the full-Muller matrix analysis of polarization, one needs a possibility to obtain several linearly-independent states of polarization using both, rotating polarizers and retarders. PSA and PSG sections have common optical elements: rotating retarders and rotating linear polarizers. Retarders and polarizers are symmetrically positioned with respect to the sample. To create and analyze the Stokes vectors for the light polarization *(S_{IN}* and *S_{OUT})* in both, PSA and PSG, we are using a combination of the rotating linear polarizers and retarders. All linear polarizers have ~ 25 mm clear aperture. The rotating analyzer ellipsometry requires linear polarizers with extinction coefficient of about 1:1000. If the extinction is worse than 1:1000, then a cumbersome correction procedure is needed for data analysis. To cover the broad spectral range between 10 and 4000 cm^{-1} with linearly polarized light we are using the following set of polarizers.

- For the frequency range between 10 and 250 cm^{-1} several free-standing wire-grid linear polarizer from SPECAC with the transmission characteristics shown in **Figure 3.1(a)** are used. There extinction ratio is between 1:2000 and 1:300. This extinction ratio is achieved by using "tandems" for linear polarizers in both PSA and PSG stages. Total of 5 polarizers are used: P0(single) to condition the synchrotron polarization, P1(tandem) to create the desired state of polarization at the sample, and P2(tandem) to analyze linear polarization. The increase of the extinction ratio at high frequencies limits application of these free-standing wire-grid polarizers for ellipsometric measurements below 250 cm^{-1}.
- Wire-grid polarizers on polyethylene substrate for frequency range between 25 and 700 cm^{-1}. Extinction ratio is 1:1000. No tandems are needed. The low-frequency limit is due to absorption in polyethylene substrate.
- KRS5 linear polarizers from SPECAC with transmission characteristics between 400 and 4,000 cm^{-1} [see **Figure 3.1(b)**]. The extinction ratio is better than 1:600. We are also using tandems in both PSG and PSA stages.

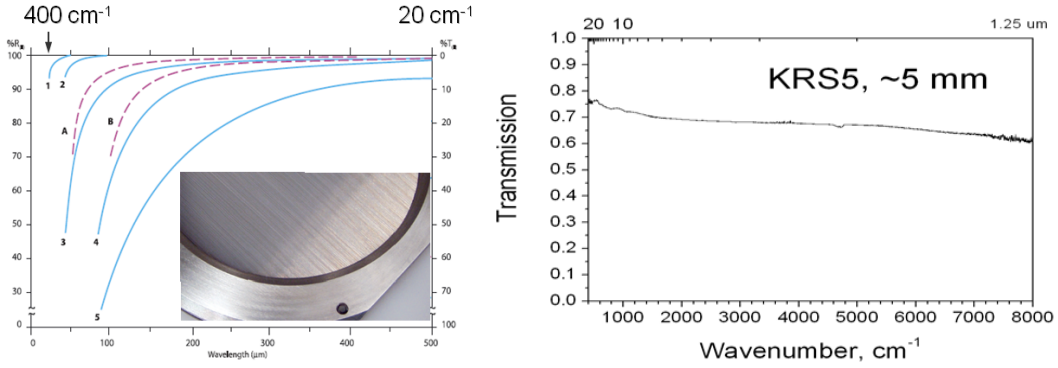

Fig. 3.1 Parameters of the linear polarizers for PSG and PSA sections.
(a) *Tp* and *Ts* characteristics of the wire grid polarizer for the frequency range between 10 and 400 cm^{-1}. The high-frequency cut-off is due to diffraction on the wires. The properties of our polarizers correspond to the curve **1**. The inset shows an image of the wire-grid polarizer.
(b) Transmission characteristic of the KRS5 polarizer in the frequency range between 400 and 6000 cm^{-1}. The low-frequency cut-off is due to the phonon absorption in KRS5 crystals.

Rotating retarders

Development of the rotating retarders for the broad frequency range is one of the main challenges of this Project. Results of this development were presented at ICSE-V [1] and published in Ref. [3]. Only basic details will be presented in this Section.

Multiple conditions have been met in this design:

1. Reasonably high transmission in the operating frequency range
2. Minimal displacement of the beam caused by the retarder rotation.

We investigated several materials systems for retarder and finally determined three types of retarders:

1. Plastic (TOPAS) retarders for operations between 10 and 100 cm^{-1}. For the clear aperture of 7.5 mm, the attenuation is between 50% at 20 cm^{-1} and 80% at 80 cm^{-1}.
2. Silicon retarders for operations between 100 and 500 cm^{-1}. Attenuation is about 90%.
3. KRS5 retarders for operations between 400 and 4,000 cm^{-1}. Attenuation characteristics have not been determined yet. Note, however, that a similar design of KRS5 retarders is used in commercial ellipsometers, so these retarders are very promising for the mid-IR spectral range.

TOPAS retarders have a composite design: Retarder consists of two triangular prisms and a small gold mirror, as shown in **Figure 3.2** and **3.4**. The behavior of the TOPAS retarder is the following: linearly-polarized radiation (after the wire-grid polarizer) enters the retarder front surface, which is normal to the beam. After the total internal reflection, the beam is directed to the gold mirror. The maximum value of the phase shift after the first internal reflection is $\pi/4$. The gold mirror with a small incident angle practically does not change the retardation. After passing the second prism, the beam is acquiring the total phase shift of $\pi/2$. Note that total retardation depends on the prism angle and the refractive index of plastic. TOPAS turns out to be a good retarder material with n=1.5 and a correspondingly low value of the back-reflection coefficient for the front surface. The kinematic mount of the small gold mirror provides the opportunity for the beam alignment inside the retarder assembly and enables the straight light propagation through the retarder. Rotation of both, linear polarizers and retarders is provided by the HUBER rotational stages [see **Fig. 3.4(a)**].

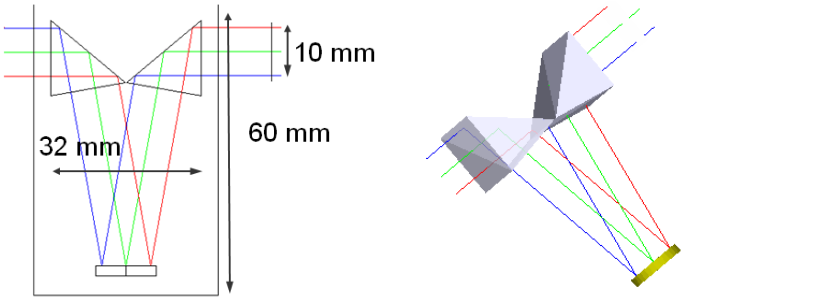

Fig. 3.2 Design of TOPAS retarder for PSG and PSA sections. (a) ZEMAX simulation for the light propagation through the TOPAS retarder consisting of two TOPAS prisms and a god mirror.
(b) 3D view for the light propagation through the retarder. Note that there is no beam displacement before and after the retarder.

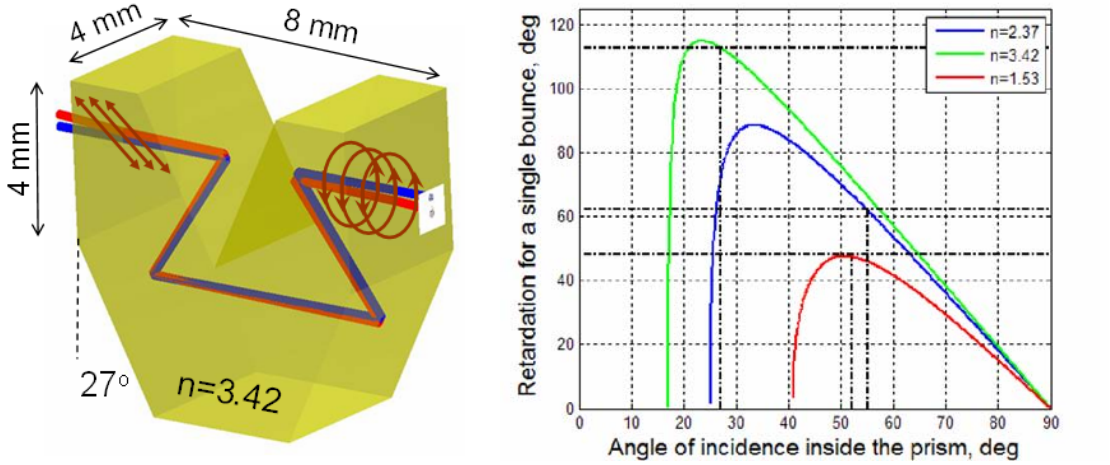

(a) (b)

Fig. 3.3
(a) ZEMAX design for a silicon double Fresnel rhomb (4 bounces) as a far infrared phase retarder with approximate dimensions that allow average transmission of ~ 10% in the frequency range between 100 and 450 cm^{-1}. Polarizations of the incoming (S2) and transmitted light (S3) are shown schematically for the left and right hand sides of the retarder respectively.
(b) The relative phase shift between *s* and *p* polarized light for a single bounce total internal reflection using far-IR average value of the refractive index of Si: n=3.42.

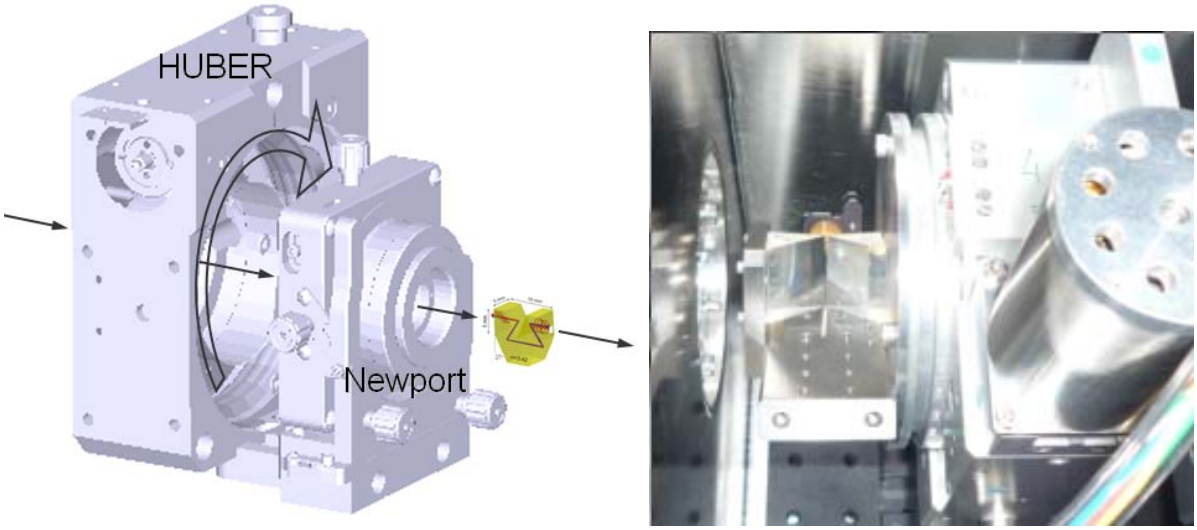

(a) **(b)**

Fig. 3.4
(a) 3D CAD design of the rotational stage assembly that enables the retarder rotation around the axis for the light propagation, thus changing the retardation angle. The assembly consists of HUBER goniometer, Newport X-Y stage, and the retarder holder (not shown). (b) TOPAS retarder inside PSA section.

The high frequency cut-off for the plastic retarders is limited by 100 cm^{-1} due to the phonon absorption. Another set of retarders made of KRS5 and Silicon will be used between 100 cm^{-1} and 4,000 cm^{-1}. Even pure Silicon shows some decline of the transmission characteristics below 100 cm^{-1} due to free-carrier absorption, which requires utilization of the aforementioned TOPAS retarder. However, between 100 and 500 cm^{-1}, Silicon provides acceptable characteristics for retardation. Above 500 cm^{-1}, the primary retarder material for us is KRS5. Both, Silicon and KRS5 retarders, have a similar double Fresnel rhomb design. The only difference between Silicon and KRS5 retarders is in the angles of the retarder planes. **Figure 3.3** show retardation calculations for TOPAS, Silicon, and KRS4 retarders, which turns out to be similar to that we have measured for the real optical components. In all cases we have parameters close to the required value of about $\pi/2$.

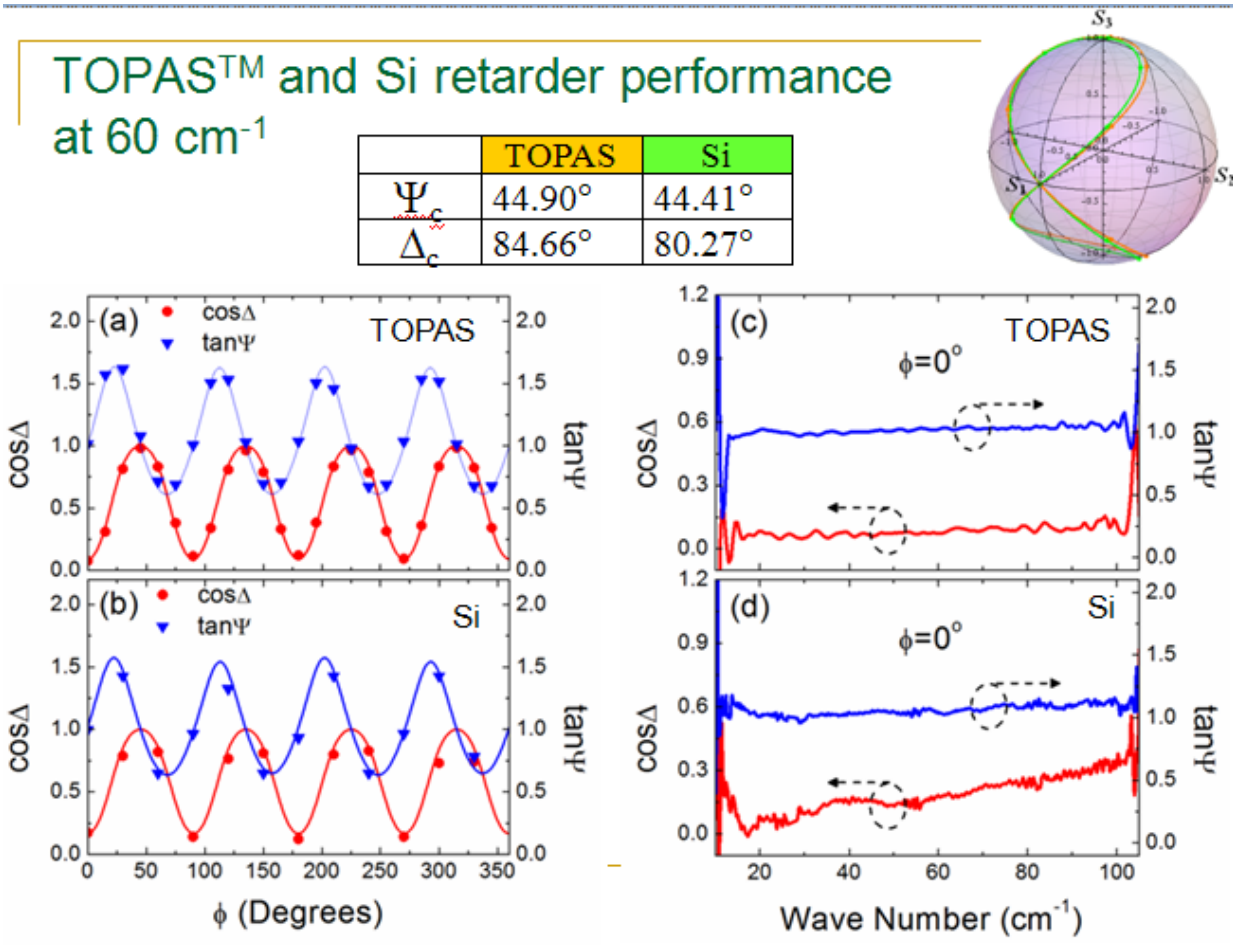

Fig. 3.5. Experimental parameters of TOPAS and Si retarders from our paper published in Ref. [3].

4. Control software: Labview Program

Standard operations of the Ellipsometer setup require a full computer control of the sample position with respect to the beam, sample temperature, as well as the position of the PSA section with respect to the sample, and the position of each polarizer and each retarder. We developed a new Labview-based program for Instrument control, calibration, and data acquisition. The outline of the Program is shown in Figure 3.1

All components of the system are controlled by a single Program. Measurements can be done in a manual regime as well as using schedules for unlimited number of internal loops and time controls. The main Program has a capability of analyzing information about the NSLS ring current and pause the measurements during the beam interruption or injection. The Labview protocol-enabled communication between the User's computer and the Local Computer fro BRUKER Interferometer will allow a possibility to use different models of BRUKER Interferometers in the future. The open code of this Program enables a possibility for the future users of

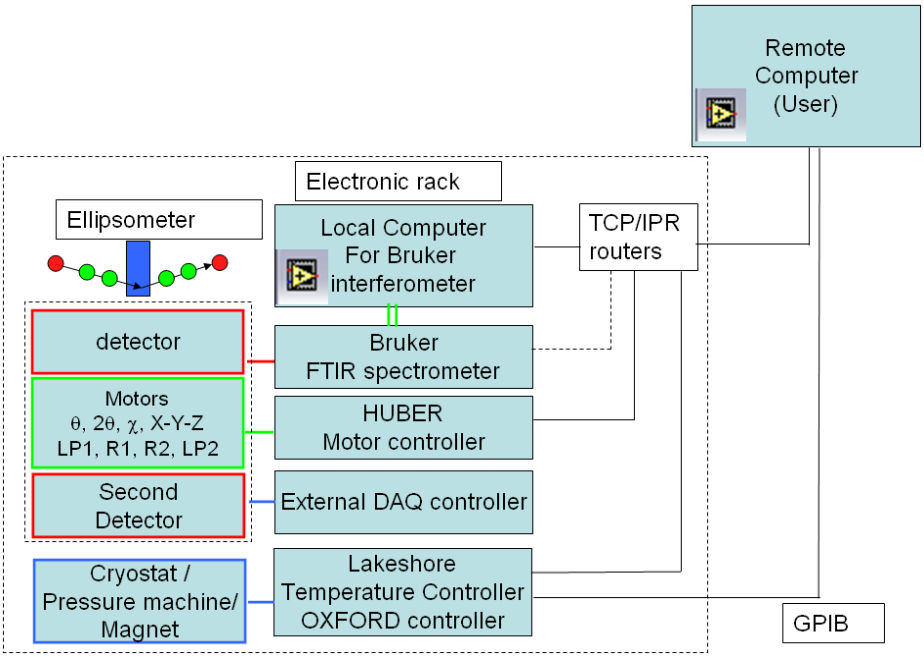

Fig. 4.1 Schematics of the instrument control Labview Program.

the instrument to upgrade and modify this Program including new Components, such as external Lasers, High Electric field, etc. This Program has been designed for us by Prof. G. Nita from NJIT Physics Department. Most of the sub-VI's have been written by Dr. T.D. Kang from our Group at NJIT.

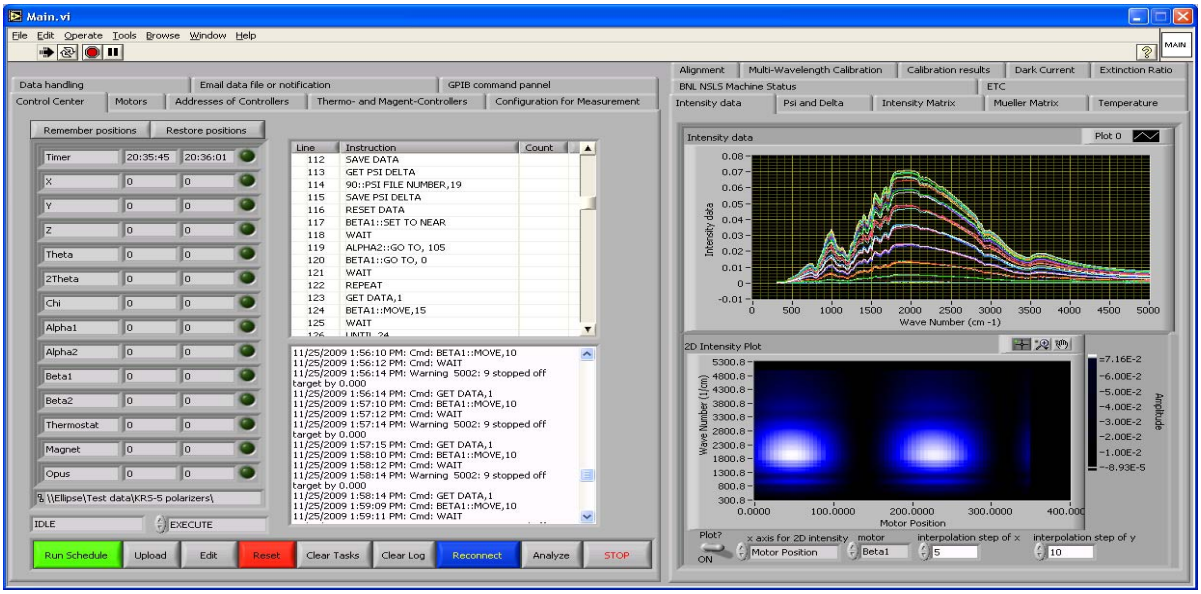

Fig. 4.2 Front panel of the instrument control Labview Program. The motor controls are at the left side, the schedule window is in the center, the Log window is under the Schedule. The current measurement window is at the right.

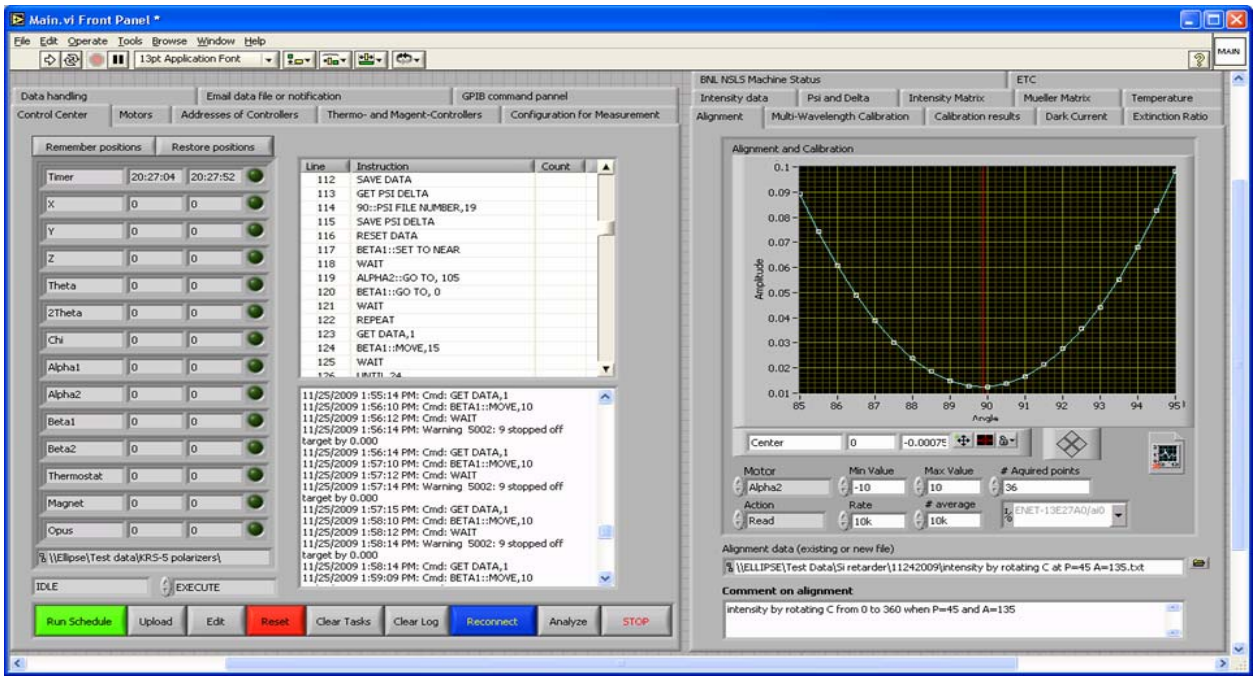

Fig. 4.3 Front panel of the polarizer-alignment window of the Labview Program. Graph at the right shows results of the polarizer alignment procedure.

5. **Data simulations and analysis / Outreach**

Traditional Transmission / Reflection spectroscopy has fundamental limitations for the study of IR excitations in strongly correlated materials. From a single transmission or reflection measurement it is impossible to determine correctly two complex functions: electric and magnetic susceptibilities:

$$\left[\hat{\varepsilon}_1(\omega)+i\cdot\hat{\varepsilon}_2(\omega) \text{ and } \hat{\mu}_1(\omega)+i\cdot\hat{\mu}_2(\omega)\right]$$

This uncertainty provides too much freedom and uncertainty for interpretation of experimental results, such as the assignment of particular excitation to magnons, phonons, or electromagnons. Even more, in multiferroic materials some excitations can be coupled, like our recently proposed ligand-field-magnon excitations [6], so their assignment to either electric- or magnetic-dipole optical transition is not unambiguous.

The aforementioned problem is a driving force for our development of the Far-IR Ellipsometer, which can measure directly all components of the dielectric and magnetic tensors and can help to identify the type of the dipole activity for the far-IR excitations. One of the key parts of any spectroscopic experiment is the possibility to simulate the expected experimental results in advance. This so-called "direct problem" is the most challenging theoretical aspect of our Project. The main challenge here is the lack of supporting literature for generalized ellipsometry in the case of anisotropic tensors for magnetic permeability and electric susceptibility. We solved this problem ourselves from basic principles. One of the Graduate Student, Paul Rogers, is working on this problem as a part of his PhD Theses. The main theoretical results of the Project are the following:

- We have developed a set of algorithms, and the corresponding MATLAB and LabView programs capable to calculate Fresnel coefficients, Jones, and Muller matrices and, the intensities for Reflectivity and Transmission spectra of the polarized radiation from bulk samples. The most general cases of anisotropic permeability and permittivity tensors, in any possible crystal symmetry and orientations have been included into consideration. As a part of the Outreach activity, we developed a website: http://web.njit.edu/~sirenko/SiMM_web/SiMM.htm, where the simulation Labview Program, SIMM4x4 is available for a free download. See **Figures 5.1 and 5.2** for illustration of this Program. SIMM4x4 has been distributed between several Research Group sat U. Maryland (Prof. Drew), U. Florida (Prof. Tanner), UC San Diego (Prof. Basov), and U. Fribourg, Switzerland (Prof. Bernhard). Short description of the Program is given below in this Section.
- We performed theoretical analysis for the Muller matrix and complex Fresnel coefficients for thin-film sample on isotropic substrate. We have demonstrated that it is indeed possible to separate dielectric and magnetic contributions into the refractive index of thin film, as well as identify whether it is a "left-handed" by performing full Mueller Matrix measurements at various AOIs. We published the main results in Ref. [2].
- The inverse problem – the capability to obtain ε(ω) and μ(ω) tensors of the sample from the measured Mueller matrix and reflection coefficients at variable incidence angles and wavelength, has been solved. See **Figure 5.3** for illustration of this fitting Program. This software can be used for data analysis either standalone, or as integrated with the LabView system control package.

SIMM4x4 Program

The basic package of SIMM4x4 Program covers MM ellipsometry experiments for semi-infinite samples with Lorentz oscillator models. Free download is here: http://web.njit.edu/~sirenko/SiMM_web/SiMM.htm
The screenshots of the Program are shown in Figures 5.1 and 5.2

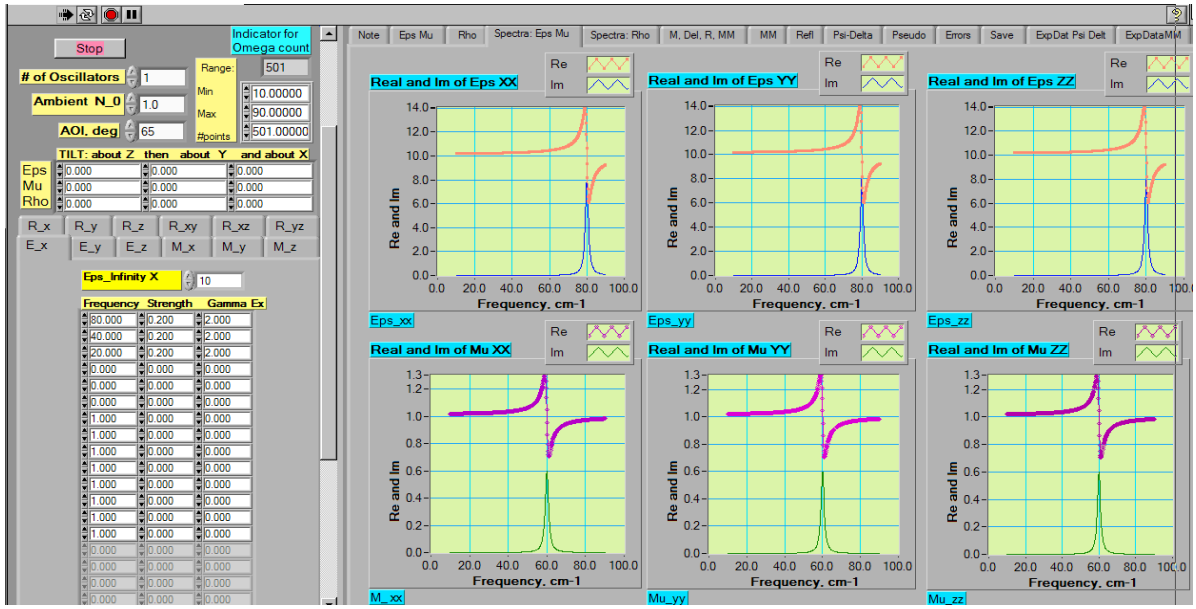

FIG. 5.1 Modeling screen of SIMM4x4 Program

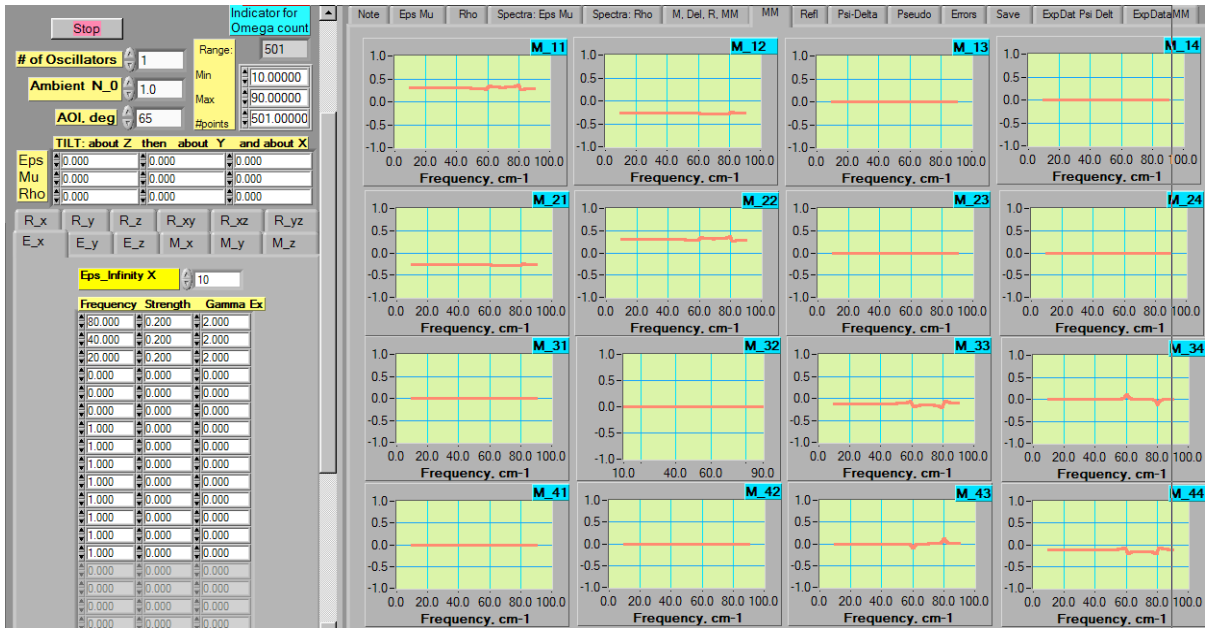

FIG. 5.2 Muller Matrix calculation screen of SIMM4x4 Program

Data fitting Program

This Program is used for fitting experimental data for the MM components and Reflectivity spectra. Parameters of the oscillators, such as the Oscillator Frequency, Oscillator Strength, and Oscillator Damping can be determined.

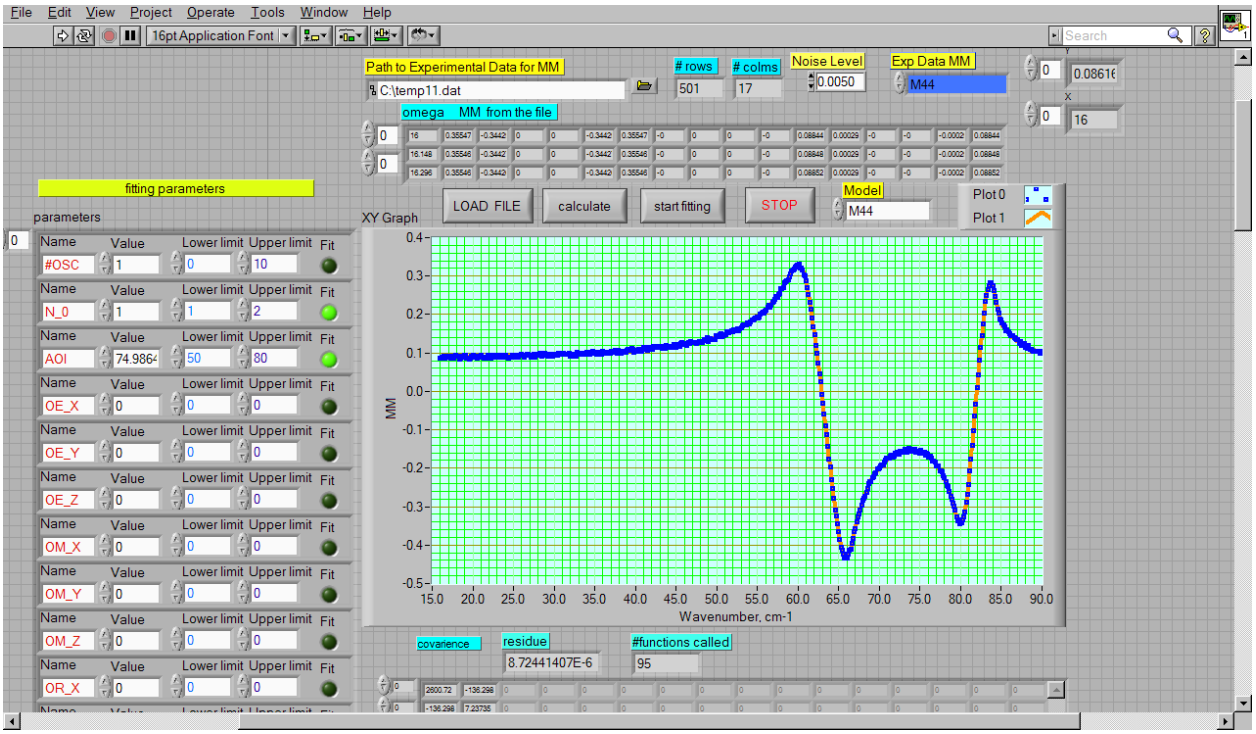

FIG. 5.3 Screen shot of the Data Fitting Program, that is based on the Levenberg–Marquardt algorithm included in the Professional Package of LabView-2010.

External Users of the Ellipsometer

Several groups of external Users applied for the beam-time to use our Ellipsometer in 2011. The general user proposals (GUP) have been submitted in October 2010. The first visits of the external Users are scheduled for February – April 2011. All groups of the outside Users have a prominent experience with ellipsometry.
The list of the outside Users:

1. Dr. Alexander Boris, Max-Planck-Institute for Solid State Research (MPI-FKF), Stuttgard, Germany, group of Prof. Keimer.
2. Prof. Stefan Zollner, New Mexico State University, Department of Physics
3. Dr. T. D. Kang, Seoul University, group of Prof. Noh. (Dr. Kang is a former Postdoc supported by the Project).

6. Theory of Operations

Traditional Mueller polarimeters for the near-IR, visible, and UV wavelength ranges use different ways of controlling and measuring polarization state: liquid crystal – based devices, that modulate retardation by switching the orientation of the fast axes of the retardation, coupled acousto- or electro- optical modulators, or by rotating polarizers and birefringent retarders. Unfortunately, none of these options is available in the far-IR range. As discussed above, we are using retarders operating by multiple internal reflections in the high-index materials: Si, TOPAS, and KRS5. The polarization states in the PSA and PSG are selected by rotating the retarders, and polarizers. Possible misalignments of our retarders may cause a significant beam displacement on the sample when retarder is rotated. Correspondingly, we choose the measurement options that minimizing such movement, especially for the retarder in the PSG.

Measurement of the Mueller matrix of the sample at each incidence angle, or sample orientation, will include collecting the reflected light intensities spectra at different combinations of orientations of the polarizer and retarder in the PSG, and polarizer and retarder in the PSA. These orientations comprise a set of {P1,C1,C2,P2} states sampled in a Mueller matrix measurements. There should be at least 16 states sampled in order to extract the 16 matrix elements of the Mueller matrix. The best choice of this set will provide the best measurement precision, and at the same time minimize movement of the retarders.

It would be preferential to implement a measurement scheme, that avoids rotating compensators altogether, but we have a proof that it is impossible to obtain all 16 Mueller matrix elements rotating only polarizers with fixed retarders.

The theory of operation and MATLAB software that allows simulating the measurement process, accounting for the component imperfections, has been developed by Dr. M.Kotelyanskii (Rudolph Technologies Inc.). Currently it implements:

1. full Mueller matrix model of the system, consisting of the Polarizer (P1), first retarder (C1), sample (S), second retarder (C2), Analyzer (P2), and detector;
2. given the parameters of retarders and sample Mueller matrix, it calculates measured intensity at the detector for a given set of angles of {P1,C1,C2,P2};
3. it allows to convert set of detector intensities measured at a number of {P1,C1,C2,P2} combinations to the sample Mueller matrix;
4. It provides an estimate of how optimal is the current set of {P1,C1,C2,P2} states from the point of view of error propagation from the measured intensities to the reported Mueller matrix.
5. This capability has been developed for both standalone use on a user's computer, and directly at the instrument, integrated with the LabView control package described in the previous Section 4.
6. Calibrations algorithms and software as discussed below.
    a. Retardation of the retarders across the spectral range
    b. Zero azimuth positions of the polarizers and retarders
    c. Retardation and transmission of the cryostat windows across the spectral range
    d. Polarization sensitivity of the detector

Light intensity at the detector I_{det} is the first component of the Stokes vector, characterizing the light incident at the detector $\mathbf{S}_{det}$, which is given by the following equation:

$$\mathbf{S}_{\text{det}} = \mathbf{P}(A)\mathbf{C}(C2)\mathbf{M}_S\mathbf{S}_{C1} = \mathbf{\Lambda}\mathbf{M}_S\mathbf{S}_{C1}$$

$$\mathbf{A} = \mathbf{P}(A)\mathbf{C}(C2); \qquad \boldsymbol{\alpha} = \begin{bmatrix} 1 \\ 0 \\ 0 \\ 0 \end{bmatrix}^{\mathbf{T}} \mathbf{A};$$

$$I_{\text{det}} = \boldsymbol{\alpha}\mathbf{M}_S\mathbf{S}_{C1}$$

Here vector $\boldsymbol{\alpha}$ – is the first row of the matrix $\mathbf{A}$. $\boldsymbol{\alpha}$ changes with different configuration of the Polarization State Analyzer (PSA). In our case PSA consists of the second retarder C2 and the analyzer A. $\mathbf{S}_{C1}$ – is the Stokes vector of light incident on the sample. $\mathbf{S}_{C1}$ changes while sampling configuration of the PSG.

To measure 16 components of the sample Mueller matrix $\mathbf{M}_s$ – at least 16 measurements of the I_{det} have to be made with different configurations of the PSG and PSA. Typically I_{det} is measured for four different configurations of the PSG, each measured with four different PSA configurations, making 16 measurements altogether. Each of the *j=1,..,4* PSG configurations will provide incident light at the sample with Stokes vector $\mathbf{S}_{C1}{}^{j}$, and each of the *i=1,…4* configurations of the PSA will be characterized by four vectors $\boldsymbol{\alpha}^{i}$. If $\mathbf{I}$ is a matrix, containing detector intensities, measured with a combination of $\boldsymbol{\alpha}^{i}$ and $\mathbf{S}_{C1}{}^{j}$, its elements are given by: $\mathbf{I}_{ij} = \boldsymbol{\alpha}^{i}\mathbf{M}_S\mathbf{S}_{C1}{}^{j}$.

Similarly, we can define a 4x4 matrix $\boldsymbol{\sigma}$ with its *j*-th column filled with $\mathbf{S}_{C1}{}^{j}$, and a 4x4 matrix $\boldsymbol{\alpha}$, with rows filled by $\boldsymbol{\alpha}^{i}$, and we can write the following equations:

$$\mathbf{I} = \boldsymbol{\alpha}\mathbf{M}_S\boldsymbol{\sigma};$$
$$\mathbf{M}_S = \boldsymbol{\alpha}^{-1}\mathbf{I}\boldsymbol{\sigma}^{-1}$$

Matrices $\boldsymbol{\sigma}$ and $\boldsymbol{\alpha}$ must have an inverse matrix, and must have ranks of at least four. This requires measurements with at least 4 different and independent states of PSA and 4 different and independent states of PSG. When there are more than 4 rows in the matrix $\boldsymbol{\alpha}$, and matrix $\boldsymbol{\sigma}$ having more than 4 columns, the inverses, can be calculated as "pseudo-inverses" in the least-squared sense. For the (pseudo-)inverses to exist, the ranks of matrices $\boldsymbol{\alpha}$, and $\boldsymbol{\sigma}$ must still equal 4. It is also important, that both $\boldsymbol{\sigma}$ and $\boldsymbol{\alpha}$ are well conditioned, so that the matrix inversion is stable, and does not amplify measurement errors.

Condition number of the matrix is defined as ratio of the largest to the smallest eigenvalues magnitudes. Matrix is close to be degenerate, and have no inverse when condition number is infinite. Condition numbers closer to 1 make results of the matrix inversion more numerically stable, and less sensitive to the errors in the measured data, rounding errors, and other perturbations. Essentially, it is a measure of linear independence of the Stokes vectors generated by the PSG, and the Stokes states sampled by the PSA.

When retarder in PSG (C1) is fixed, it turns out that matrix σ has zero determinant, no matter what the *C1*, or *P* values are, and therefore it is impossible to measure all 16 components of the sample Mueller matrix without rotating the retarder. The best condition numbers for σ are achieved when rotating retarders across the range of 0 to 90, as is common in typical UV-near IR systems, but this would maximize the possible beam displacement in the far-IR system. We found however, that it is possible to obtain acceptable condition numbers for σ by moving retarders only within the ±15 degrees range.

Further development for the Theory of Operation, which is in progress now, will include

- user interface for error analysis by simulating effects of the component imperfections,
- developing user interface to analyze the system measurement errors, and to identify the most favorable set of the PSA and PSG sampling states for a given measurement.

REFERENCES

[1] T. D. Kang, P. Rogers, E. Standard, G. M. Nita, T. Zhou, G. L. Carr, S. Zollner, M. Kotelyanskii, and A. A. Sirenko**, "***Far-infrared Mueller Matrix Ellipsometer at the National Synchrotron Light Source"*, Invited talk at ICSE-V, Albany, USA, May 23rd - 28th, 2010.

[2] P. D. Rogers, T. D. Kang, T. Zhou, M. Kotelyanskii, and A. A. Sirenko, "*Mueller matrices for anisotropic metamaterials generated using 4×4 matrix formalism*", Thin Solid Films (2011), doi:10.1016/j.tsf.2010.12.066.

[3] T. D. Kang, E. Standard, G. L. Carr, T. Zhou, M. Kotelyanskii, and A. A. Sirenko, "*Rotatable broadband retarders for far-infrared spectroscopic ellipsometry*", Thin Solid Films, (2011), doi:10.1016/j.tsf.2010.12.057.

[4] P. D. Rogers, Y. J. Choi, E. Standard, T. D. Kang, K. H. Ahn, A. Dudroka, P. Marsik, C. Bernhard, S. Park, S-W. Cheong, M. Kotelyanskii, and A. A. Sirenko, submitted to Phys. Rev. Lett. (2011). arXiv:1101.2675v1 [cond-mat.str-el]

[5] http://www.nsls.bnl.gov/beamlines/beamline.asp?blid=U4IR

[6] T. D. Kang, E. Standard, K. H. Ahn, and A. A. Sirenko, G. L. Carr, S. Park, Y. J. Choi, M. Ramazanoglu, V. Kiryukhin, and S-W. Cheong, "*Coupling between magnon and ligand-field excitations in magnetoelectric $Tb_3Fe_5O_{12}$ garnet*", Phys. Rev. B **82**, 014414 (2010).